

## Paper-Based Electrical Respiration Sensor

Firat Güder, Alar Ainla, Julia Redston, Bobak Mosadegh, Ana Glavan, T. J. Martin, and George M. Whitesides\*

**Abstract:** Current methods of monitoring breathing require cumbersome, inconvenient, and often expensive devices; this requirement sets practical limitations on the frequency and duration of measurements. This article describes a paper-based moisture sensor that uses the hygroscopic character of paper (i.e. the ability of paper to adsorb water reversibly from the surrounding environment) to measure patterns and rate of respiration by converting the changes in humidity caused by cycles of inhalation and exhalation to electrical signals. The changing level of humidity that occurs in a cycle causes a corresponding change in the ionic conductivity of the sensor, which can be measured electrically. By combining the paper sensor with conventional electronics, data concerning respiration can be transmitted to a nearby smartphone or tablet computer for post-processing, and subsequently to a cloud server. This means of sensing provides a new, practical method of recording and analyzing patterns of breathing.

**R**ate of respiration, together with heart rate, blood pressure and body temperature, is used by healthcare workers to estimate the basic health-status of patients.<sup>[1]</sup> In differentiating between stable and unstable patients, the rate of respiration is a better metric than other vital signs.<sup>[2]</sup> Abnormalities in the rate and pattern of respiration are a strong predictor of acute events, such as cardiac arrest, or for characterizing illnesses, such as chronic obstructive pulmonary disease (COPD), pneumonia, and asthma.<sup>[3]</sup>

The respiratory rate of a healthy adult at rest is 12–20 breaths per minute, and corresponds to an exchange of six–eight liters of air per minute.<sup>[4]</sup> Fieselmann et al. reported that a rate of respiration greater than 27 breaths per minute was the most important predictor of cardiac arrest in hospital wards.<sup>[5]</sup> Cretikos et al. observed that, in the general wards, patients suffering from a serious illness, and having a rate of respiration greater than 24 breaths per minute, could be identified as high risk (for intervals up to 24 hours), with a specificity of 95%.<sup>[2]</sup> Continuous measurement of the rate and depth of respiration during sleep is also important in

diagnosing sleep apnea, a condition estimated to affect 25 million Americans, 80% of whom remain undiagnosed.<sup>[6]</sup>

In addition to being an important metric for characterizing health, the rate of respiration is a reliable marker for determining the anaerobic threshold (AT), also known as the lactate threshold, in athletes.<sup>[7]</sup> AT is defined as the highest level of exercise that can be maintained without inducing metabolic acidosis;<sup>[8]</sup> this level is strongly associated with athletic performance.

In most clinical settings, (e.g. the emergency room of a hospital), the rate of respiration is commonly measured by observing the patient from a distance, and counting the rising and falling of the chest.<sup>[9]</sup> Although this method is simple, it is subjective, and provides little, if any, information about the depth of respiration of the patient. It is also challenging and impractical to monitor individual patients visually over extended periods of time.<sup>[10]</sup>

Dedicated biomedical instruments accurately monitor the rate of respiration. These instruments usually use the sound, airflow, and movement of the chest,<sup>[11]</sup> with airflow being the most commonly used in clinics. A temperature sensor (e.g. thermistor) is typically used for detection, since exhaled air is usually warmer than the inhaled air, and the cyclical change in temperature can be transduced and correlated with a rate of respiration.<sup>[12]</sup> This method, however, is prone to errors due to unintentional displacement of the (rigid) sensor during measurement.

Other technologies measure respiratory activity using a pressure sensor.<sup>[13]</sup> In this method, an increase in pressure is registered by the sensor when the subject exhales air. The main drawback of this method is the heavy, non-flexible facemask/mouthpiece or the uncomfortable nasal cannula that the subject must wear. These instruments are also expensive: more than \$150 without the reader electronics (the components that digitize the recorded analog signal and display the results) and several thousand dollars as a complete system; this cost limits the use of this type of device. Detection of the rate of respiration based on sound using acoustic sensors, such as microphones, has been suggested as an alternative.<sup>[14]</sup> This form of transduction, however, performs poorly when the patient coughs/sneezes, snores or cries (in case of infants) or is in a noisy surrounding. Capnography is another important but expensive method for monitoring respiration (including the rate of respiration), particularly in the context of anesthesia, emergency medicine, intensive care units, and sleep medicine.<sup>[15]</sup>

This article reports an effective, simple, inexpensive sensor for monitoring respiration. The sensor is capable of measuring the rate of respiration of a person by detecting the transient difference in moisture adsorbed on paper from inhaled and exhaled air. The sensor comprises a piece of

[\*] Dr. F. Güder, Dr. A. Ainla, J. Redston, Prof. B. Mosadegh, Dr. A. Glavan, T. J. Martin, Prof. G. M. Whitesides  
Department of Chemistry and Chemical Biology  
Harvard University  
12 Oxford Street, Cambridge, MA 02138 (USA)  
E-mail: gwhitesides@gmwgroup.harvard.edu  
Prof. B. Mosadegh, Prof. G. M. Whitesides  
Wyss Institute for Biologically Inspired Engineering  
Harvard University  
60 Oxford Street, Cambridge, MA 02138 (USA)

Supporting information for this article can be found under:  
<http://dx.doi.org/10.1002/anie.201511805>.

paper with digitally printed graphite electrodes, and is attached inside a flexible textile procedure mask (commonly used in hospitals; see Figure 2). In our current design, it includes a battery-powered unit that can interface with an internet-enabled tablet computer/smartphone. This system can display and upload the collected data to the cloud, and thus enable remote access to the results. The paper sensor, electronics, and software, essentially transform a simple textile mask into a functional mask (with internet connectivity), which can measure, analyze, store, and share information concerning the rate and pattern of respiration of individual patients.

The paper sensor exploits the hygroscopic character of cellulose paper—that is, its tendency to adsorb water from the environment. For instance, at a relative humidity (RH) of 70%, paper absorbs up to 10% of its weight in water. Since the ionic conductivity of the paper is proportional to the amount of water on the surface of the cellulose fibers, the changes in moisture content of paper due to breathing can be used to monitor respiration.<sup>[16]</sup>

When breathing out, human breath is fully humidified (RH 100%), and therefore, increases the amount of water on the sensor, and thus its ionic conductivity. When breathing in, the amount of water on the surface of the cellulose fibers is reduced because the surrounding atmosphere almost always has a lower RH than the exhaled air. This change in the amount of adsorbed water decreases the ionic conductivity of the sensor (Figure 1). Essentially, the paper sensor transduces variations in the level of moisture of its immediate surrounding to an electrical signal. Using this device, we can acquire

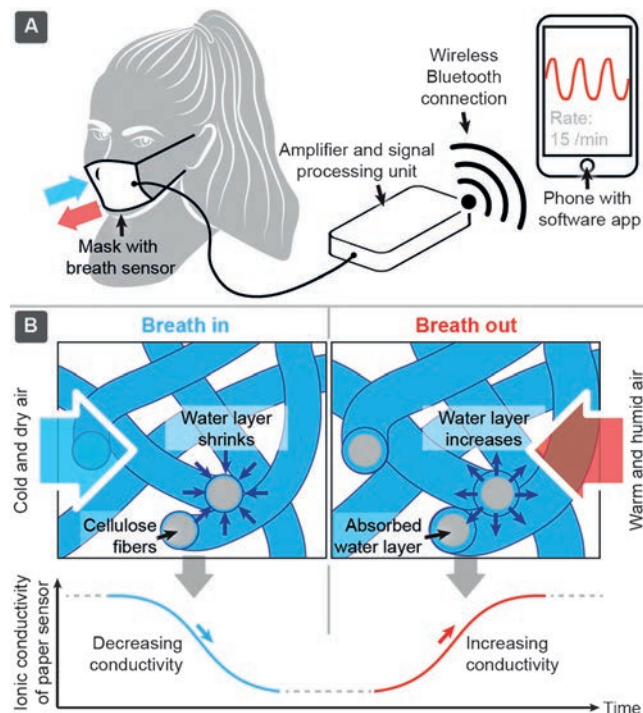


**Figure 1.** A) Schematic illustration of the facemask for respiration monitoring with the embedded paper-based sensor and electronics. B) Mechanism of operation of the paper-based electrical respiration sensor.

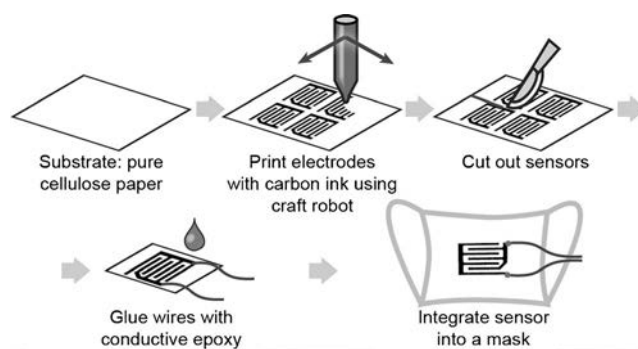


**Figure 2.** Schematic illustration of the fabrication of digitally printed paper sensors with graphite ink.

the rate and pattern of respiration of a person accurately. As the sensor itself measures transient changes in moisture content between the inspired and expired air, the system requires no calibration.

The paper sensors were fabricated by digitally printing graphite ink (Ercon Graphite Ink 3456) using a ball-point pen and a craft cutter/printer (Graphtec Craft Robo Pro) onto paper.<sup>[17]</sup> The graphite ink was diluted with a proprietary solvent (Ercon ET160) 55:45 w/w to obtain a desired consistency for printing, and the mixture was homogenized using a tip sonicator to create a uniform dispersion. Using this printing technique, large numbers of sensors can be printed with high accuracy (see Figure S1 in the Supporting Information). (Other printing techniques such as screen printing or reel-to-reel printing can also be used for increased throughput). We chose an interdigitated electrode design to increase the area of the electrodes and the signal-to-noise ratio. This design also allows rapid access of humid air to the paper. We have also produced sensors with electrodes located on the top and bottom surface of the paper (Figure S2). The power required for this design of the sensor is 250  $\mu\text{W}$  at a RH of 90%, which is similar to the power requirement of the interdigitated design (175  $\mu\text{W}$ ) at the same RH. Due to slightly higher complexity in fabrication, we fabricated sensors with the interdigitated design for convenience. For more information about the characterization of the sensors, the mask used in the experiments, electronics and software, see the Supporting Information.

The moisture content of paper is a function of the relative humidity of the surrounding environment.<sup>[16a,b]</sup> Figure S3 shows the electrical conductivity of the paper-based moisture sensors, fabricated from different types of paper, over a range of RH (0–90% RH). We performed these electrical measurements by applying a 25V DC potential across the graphite electrodes, and measuring the resulting current. We chose 25V to obtain a high signal-to-noise ratio. Currents less than 1 nA had a poor signal-to-noise ratio and were not used.

We explored three different kinds of papers (Figure S3) for the fabrication of the paper sensors: 1) Whatman 1 Chr, 2) Whatman 3MM Chr, and 3) copy paper. Both Whatman 1 Chr and Whatman 3MM Chr papers are made of pure cotton cellulose fiber with a basis weight of 87  $\text{g m}^{-2}$  and 185  $\text{g m}^{-2}$ . (The basis weight of paper is defined as the weight of paper per unit area).<sup>[18]</sup> The standard copy paper had

a basis weight of  $80 \text{ g m}^{-2}$ . None of the sensors fabricated from these papers generated a readable current below a RH of 20%. Whatman 1 Chr had the lowest sensitivity, and did not produce a distinguishable signal below a RH of 65%. Whatman 3MM Chr was significantly more sensitive than Whatman 1 Chr, and detected all levels of  $\text{RH} > 30\%$  (Figures S4–S6 describes the magnitude of hysteresis, batch-to-batch variations on the sensor output, and analysis of response times of the sensors). The difference in sensitivity between sensors fabricated with Whatman 3MM Chr and Whatman 1 Chr may be due to their basis weight. A larger area of cellulose fibers in a given area of paper would create a greater number of electrically conductive pathways at a given level of RH (i.e., reducing the overall resistivity) and thus increasing the sensitivity of the sensor. The copy paper showed the highest sensitivity. The mechanism of this difference is not presently known, but is not important for the function of the sensor. The high sensitivity of the copy paper compared to Whatman 3MM Chr came at the cost of a 10 times higher power consumption for the sensor. We, therefore, used Whatman 3MM Chr for the majority of the experiments.

The sensor is a simple two-electrode electrochemical cell, in which water (from atmosphere or breath) is electrolyzed on the application of an electrical potential between the electrodes. The corresponding oxidation and reduction reactions of water on the surface of the two graphite electrodes produce a measurable electrical current. We expect the only electrolysis products to be small quantities of  $\text{O}_2$  and  $\text{H}_2$ .

We observed only a weak dependence of the output current of the paper sensor on the temperature (between  $22^\circ\text{C}$  and  $40^\circ\text{C}$ ; Figure S7). We attribute this small difference to an increase in the mobility of ions at elevated temperatures, and thus an increase in conductivity.<sup>[16b]</sup> The observed difference, however, was small enough (20% at RH 90%) to neglect.

We also verified that the paper sensor is not sensitive to  $\text{CO}_2$  (see Figure S8) up to a mole fraction in the gas flowing through the sensor of 25%. We presume this insensitivity is due to the low solubility of  $\text{CO}_2$  in water ( $< 0.5 \text{ g L}^{-1}$ , room temperature, 1 atm).<sup>[20]</sup> The paper sensor is, therefore, primarily sensitive to changes in the amount of moisture adsorbed on the paper, and the electrical signal is not affected by the concentration of  $\text{CO}_2$  in human breath ( $< 5\%$ ).

The electrical conductivity of paper can be modified by the addition of ionic species that increase the concentration of charge carriers, and thus, increase the magnitude of ionic current between the electrodes. Widely available water-soluble ionic compounds, such as salts, make it possible to tune the electrical properties of the paper sensor (Figures S9 and S10).

We placed pure cellulose paper-based moisture sensors, with no added salts, in textile procedure masks to demonstrate their use with healthy adults (seven members of our research team—Figure 3a).

We designed and fabricated a simple device for data acquisition using off-the-shelf electronic components (Figure 3b). This instrument generated a 25 V DC potential from a 5 V DC power source, and applied the voltage across the

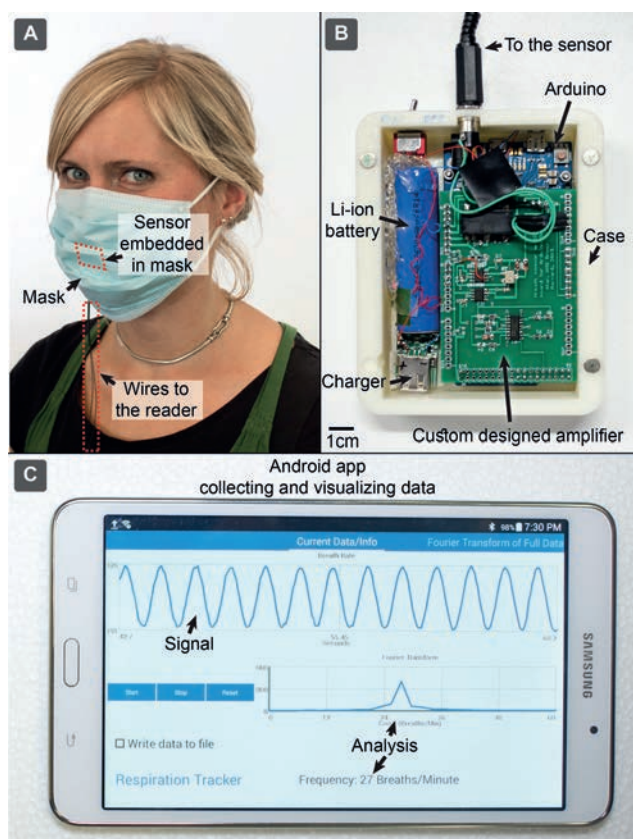


**Figure 3.** A) The facemask with the embedded paper-based sensor. B) Photograph of the data acquisition electronics with Li-ion batteries, Arduino microcontroller board, custom designed amplifier board, and 3D printed casing. C) Photograph of tablet computer running the Android app, which can display and analyze the incoming data stream from the data acquisition electronics.

electrodes of the paper sensor. The unit amplified and digitized the resulting electrical current, and transmitted the data to a tablet computer (Figure 3c) over a wireless Bluetooth communication link. The custom-built Android application, with a minimally complex design, displayed the incoming data and ran simple analytics (e.g. Fourier transformations; first derivatives). The software could also save the collected results to a text file, which could be uploaded to the cloud, or emailed to a third party for off-site analysis. This feature would be particularly useful for individuals who might monitor their respiration at home, and wish to share their results remotely.

The Android application also has the option to apply finite-impulse-response (FIR) and infinite-impulse-response (IIR) digital filtering algorithms to the acquired signal.<sup>[21]</sup> Digital filters are commonly used for the separation of combined signals and the restoration of distorted (i.e. noisy) signals. Since the system we described can be used as a research tool, the user has the flexibility to design custom digital filters (e.g. low-pass, high-pass, band-pass, band-stop) to extract other metrics from the recorded pattern of respiration. The filter coefficients can be stored as a text file on the tablet computer and imported when the application is launched. Both the filtered and the raw data are recorded as

a text file for later analysis. By implementing additional compressed sensing/ sparse sampling algorithms, the size of the files containing the collected data can be made significantly smaller, to enable use of networks with low speeds. This capability is required in the developing world.<sup>[22]</sup>

The functional textile mask was able to track the respiratory activity of the subjects successfully up to 15 minutes at room temperature (Figure 4a and Figures S11–S16) while at rest (i.e. sitting in a chair); the duration of the experiment was limited by the specifications

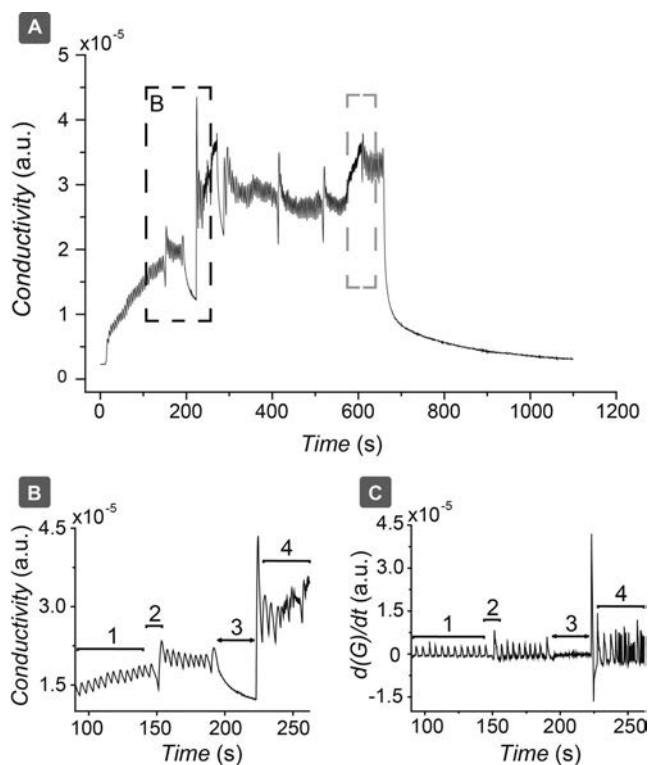


**Figure 4.** A) The resting respiratory activity of a subject recorded using the functional facemask. We asked the subject to breathe normally, take deep breaths, pause and breathe randomly during the experiment. B) Unprocessed breathing patterns recorded while: 1. breathing normally, 2. taking a deep breath, 3. paused and, 4. random breathing. C) The first derivative of the breathing patterns shown in (B;  $G$  denotes conductivity); eliminates the drifting baseline and sharpens the peaks.

of the Institutional Review Board (IRB) approval under which we worked. There is a significant initial drift in the output of the paper sensor. The drift probably reflects the large difference in drying and humidifying cycles during breathing, and reaches equilibrium in a few minutes. Since, however, we are primarily interested in measuring the intervals between the signal maxima, the change in the absolute level of signal caused by the drift is not relevant. Figure 4b displays different breathing patterns acquired during a representative experiment with a single subject. The area marked with (1) is a normal breathing pattern (which consists of periodic breathing cycles of similar magnitude) followed by a deep breath marked as (2).

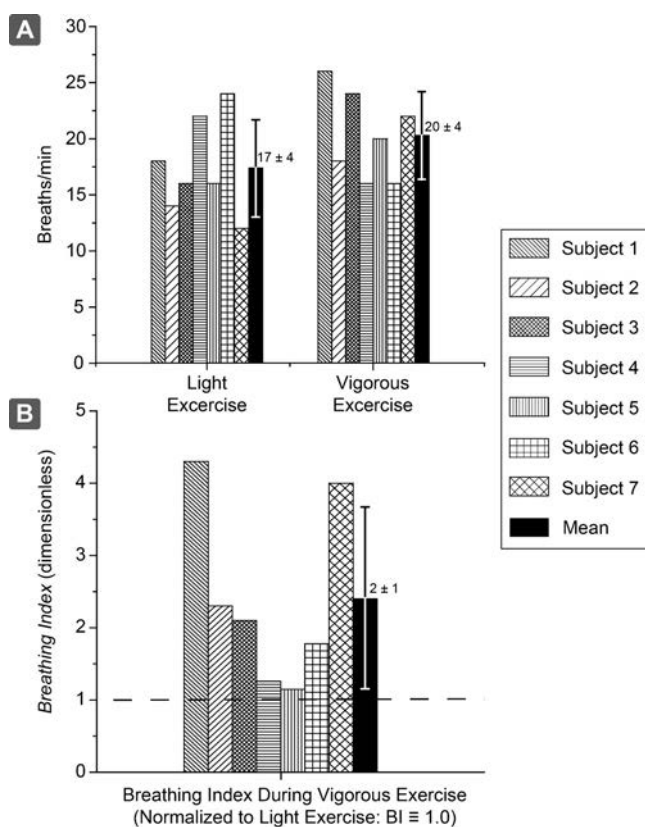
During this period, the subject had a rate of respiration of 14 breaths per minute. A pause in breathing was registered as a drop in the recorded output current (3). A mixture of deep, slow, fast, and shallow breathing patterns could also be accurately monitored during the experiment and marked as (4) in Figure 4b. The drifting baseline can be eliminated by taking the first derivative of the signal, which is equivalent to high-pass filtering of the respiratory signal (Figure 4c). The processed signal also has sharper peaks, and thus renders visual analysis easier. The device responded seamlessly to the transition between periods of fast, shallow and normal breathing as highlighted with a grey dashed box in Figure 4a (see Figure S17 for a close-up view). The system was also able to acquire and transmit all of the collected data to the tablet computer.

Figure S18 shows one of the trials (Figures S19–S24 for data from the rest of the trials) in which a subject took a short walk inside the building to test two performance factors of the system: i) noise levels in the data collected during movement, and ii) system performance during light exercise (i.e. walking around the hallways) and vigorous exercise (i.e. high tempo climbing of four flights of stairs in the building). The recorded data had little observable noise during both light exercise (Figure S18b) and vigorous exercise (Figure S18c); the rate of respiration could easily be detected by counting the number of peaks. The subject registered a rate of respiration of 12 breaths  $\text{min}^{-1}$  during light exercise, and 22 breaths  $\text{min}^{-1}$  during more vigorous exercise. (The breath counts were calculated manually from the collected data). Interestingly, some of the subjects (Figure S19) decreased their rate of respiration when transitioning from light exercise (24 breaths  $\text{min}^{-1}$ ) to vigorous exercise (16 breaths  $\text{min}^{-1}$ ). These subjects compensated for the decrease in rate of respiration by taking deeper breaths (Figures S19b and S19c). Figure 5a summarizes the rate of respiration of each subject during light and vigorous exercise.

To provide an additional metric (one related to the respired volume) for the respiration of subjects, we analyzed the amplitude of the signal generated by the sensor. The amplitude of the signal correlates with the depth of breathing by the subject. When a subject transitions from light exercise to vigorous exercise, two parameters related to respiration may change: 1) the rate of respiration (RR), which can be calculated by counting the number of peaks of the captured cyclic signal in a measured interval of time, and 2) the depth of respiration (DR), which we assume to correlate (undoubtedly non-linearly) the peak-to-peak amplitude of the train of breaths captured by the device. We defined an empirical metric, the breathing index (BI) by Equation (1) (see Figure S25 for more details on BI).

$$\text{BI} = \left( \frac{\text{RR}_{\text{Vigorous}}}{\text{RR}_{\text{Light}}} \right) \times \left( \frac{\text{DR}_{\text{Vigorous}}}{\text{DR}_{\text{Light}}} \right) \quad (1)$$

Here,  $\text{RR}_{\text{Vigorous}}$  is the rate of respiration during vigorous exercise,  $\text{RR}_{\text{Light}}$  is the rate of respiration during light exercise,  $\text{DR}_{\text{Vigorous}}$  is the peak-to-peak amplitude of the signal during vigorous exercise, and  $\text{DR}_{\text{Light}}$  is the peak-to-peak amplitude of the signal during light exercise. This approach leads to the



**Figure 5.** Summary of the rate of respiration A) of each subject during light and vigorous exercise. B) The Breathing Index of each subject during vigorous exercise (normalized to light exercise). Although some subjects exhibited an increasing or decreasing rate of respiration when transitioning from light exercise to vigorous exercise, most of the subjects respired a higher volume of air during vigorous exercise than light exercise, as indicated by a BI > 1. (Error bars represent standard deviations for  $N = 7$ ).

obvious conclusion that all of the subjects exchanged a larger volume of air during vigorous exercise ( $BI > 1$ ) than they did during light exercise (Figure 5b), a conclusion that cannot be derived solely from the rate of respiration. Our analysis indicated that Subject 5 is more fit than Subject 1, since Subject 5 has the lowest breathing index among all participants in the experiment.

Overall, the paper sensor, electronics and the mobile app, performed without failure or interruption of data during the experiments, and thus have the potential to be used for monitoring breathing, both at rest and during physical activity. An inexperienced individual could learn how to read and interpret these graphs within a few minutes. Filtering out the drifting baseline using digital filters would further simplify the process of manual interpretation.

In conclusion, the paper-based electrical respiration sensor is sufficiently low-cost (\$0.005 for materials for the paper chip and \$1.50 for the mask) that it can be considered for single-use applications. It enables continuous monitoring of the respiratory activity (up to 60 breaths  $\text{min}^{-1}$ ) for a number of populations (e.g., patients, athletes, research subjects, smokers, perhaps children). The information is obviously less accurate than that available in a pulmonology

laboratory, but is more convenient and perhaps more useful in routine and at-home monitoring. We believe this sensor will be (at least initially) most immediately useful in characterizing sleep apnea. In addition, we believe athletes, or others to whom fitness is important, might use this sensor to monitor breathing to track changes in their performance. Our platform can also be extended to or combined with other emerging and existing technologies to detect and measure gas phase analytes other than water.<sup>[23]</sup>

The system has three limitations: 1) The power requirement for electronics is too high for intervals of use up to a full day on a single charge of the battery (although it should be adequate for one complete night of sleep: the current design can run for 9 h on a single charge using a 18650 type lithium-ion battery with a nominal capacity of 2600 mAh); the data acquisition system requires daily charging of its batteries. Full day or week monitoring would require more battery capacity. 2) The electrodes of the sensor are prone to cracking if the paper is folded, but folding should not occur during regular use of the sensor. 3) We expect the paper sensor may not work efficiently, or at all, at temperatures  $< 0^\circ\text{C}$  due to freezing of the moisture and build-up of ice inside the paper. We expect that the performance of the sensor would also be reduced on a day with RH 100% at  $37^\circ\text{C}$ . Such conditions are, however, uncommon.

The paper-based respiration sensor, combined with conventional electronics, is capable of collecting and sending respiration data to a tablet computer or a smartphone using wireless connectivity. The custom-built Android app running on the tablet computer/smartphone has the ability to run simple analytics (e.g. Fourier transforms) on the incoming data stream, and apply digital filtering algorithms for signal processing. Both the raw and the filtered data can be uploaded to the cloud and shared with a healthcare professional with the click of a button, thus eliminating unnecessary visits to the clinic. This system is non-invasive, and thus allows physical scientists access to physiologically relevant human data under simple IRB approvals. Operation is sufficiently simple that inexperienced, first-time users can be trained in a matter of a few minutes; all they have to do is to put on the mask, run the Android app and click on “start” in order to monitor and record respiration.

We obtained written consent from all subjects who participated in the experiments. The research protocol and all associated materials were approved by the Harvard University, Faculty of Arts and Sciences, Institutional Review Board (IRB) under the reference number IRB15-0949.

### Acknowledgements

This work was funded by DTRA (contract number HDTRA1-14-C-0037). The research of F.G. is sponsored by the German Research Foundation—DFG (contract number GU 1468/1-1). A.A. thanks the Swedish Research Council for financial support. We would like to thank Mr. Jim McArthur and the Electronic Instrument Design Lab (Department of Physics, Harvard University) for assistance in fabrication of

electronics. We would also like to thank Victoria Campbell, Chien-Chung Wang, K.C. Liao, Nicolas Fulleringer, Sergey Semenov, Philipp Rothemund, Mahiar Hamed, Baris Unal, and Robert Kacmarek for fruitful discussions.

**Keywords:** digital health · internet of things · paper · respiration · sensors

**How to cite:** *Angew. Chem. Int. Ed.* **2016**, *55*, 5727–5732  
*Angew. Chem.* **2016**, *128*, 5821–5826

- [1] a) R. Parkes, *Emerg. Nurse* **2011**, *19*, 12–17; b) Z. V. Edmonds, W. R. Mower, L. M. Lovato, R. Lomeli, *Ann. Emerg. Med.* **2002**, *39*, 233–237.
- [2] M. A. Cretikos, R. Bellomo, K. Hillman, J. Chen, S. Finfer, A. Flabouris, *Med. J. Aust.* **2008**, *188*, 657.
- [3] M. Woollard, I. Greaves, *Emerg. Med. J.* **2004**, *21*, 341–350.
- [4] W. F. Ganong, K. E. Barrett, *Review of Medical Physiology, Vol. 21*, McGraw-Hill Medical, New York, **2005**.
- [5] J. F. Fieselmann, M. S. Hendryx, C. M. Helms, D. S. Wakefield, *J. Gen. Intern. Med.* **1993**, *8*, 354–360.
- [6] a) D. Noonan, *Sci. Am.* **2015**, *312*, 27–28; b) P. E. Peppard, T. Young, J. H. Barnet, M. Palta, E. W. Hagen, K. M. Hla, *Am. J. Epidemiol.* **2013**, *177*, 1006–1014; c) A. S. Gami, D. E. Howard, E. J. Olson, V. K. Somers, *N. Engl. J. Med.* **2005**, *352*, 1206–1214; d) P. J. Strollo et al., *N. Engl. J. Med.* **2014**, *370*, 139–149.
- [7] a) D. G. Carey, G. Pliego, R. Raymond, *J. Exerc. Physiol.* **2008**, *11*, 44–51; b) D. G. Carey, L. A. Schwarz, G. J. Pliego, R. L. Raymond, *J. Sports Sci. Med.* **2005**, *4*, 482.
- [8] R. B. George, M. A. Matthay, R. W. Light, R. A. Matthay, *Chest Medicine: Essentials of Pulmonary and Critical Care Medicine*, Lippincott Williams & Wilkins, Philadelphia, **2005**.
- [9] W. Karlen, H. Gan, M. Chiu, D. Dunsmuir, G. Zhou, G. A. Dumont, J. M. Ansermino, *PLoS One* **2014**, *9*, 99266.
- [10] M. Folke, L. Cernerud, M. Ekström, B. Hök, *Med. Biol. Eng. Comput.* **2003**, *41*, 377–383.
- [11] F. Q. Al-Khalidi, R. Saatchi, D. Burke, H. Elphick, S. Tan, *Pediatr. Pulmonol.* **2011**, *46*, 523–529.
- [12] K. Storck, M. Karlsson, P. Ask, D. Loyd, *IEEE Trans. Biomed. Eng.* **1996**, *43*, 1187–1191.
- [13] a) R. G. Norman, M. M. Ahmed, J. A. Walsleben, D. M. Rapoport, *Sleep* **1997**, *20*, 1175–1184; b) T. L. Lee-Chiong, *Sleep: a comprehensive handbook*, Wiley Online Library, **2006**.
- [14] a) L. Autet, D. Frasca, M. Pinsard, A. Cancel, L. Rousseau, B. Debaene, O. Mimoz, *Br. J. Anaesth.* **2014**, *113*, 195–197; b) Y. Guechi, A. Pichot, D. Frasca, F. Rayeh-Pelardy, J.-Y. Lardeur, O. Mimoz, *J. Clin. Monit. Comput.* **2015**, 1–6 (Available Online DOI: 10.1007/s10877-10015-19658-y); c) H. Jin, L. Lee, L. Song, Y. Li, J. Peng, N. Zhong, H. Li, X. Zhang, *J. Clin. Sleep Med.* **2015**, *11*, 765–771.
- [15] a) N. Jaimchariyatam, R. A. Dweik, R. Kaw, L. S. Aboussouan, *J. Clin. Sleep Med.* **2013**, *9*, 209; b) S. Yamamori, Y. Takasaki, M. Ozaki, H. Iseki, *J. Clin. Monit. Comput.* **2008**, *22*, 209–220; c) M. L. Langan, J. C. Kurtz, P. Schaeffer, A. G. Asnes, A. Riera, *J. Crit. Care* **2014**, *29*, 1035–1040; d) C. Weihu, Y. Jingying, H. Demin, Z. Yuhuan, W. Jianguyong, *Am. J. Otolaryngol.* **2011**, *32*, 190–193.
- [16] a) D. Tobjörk, R. Österbacka, *Adv. Mater.* **2011**, *23*, 1935–1961; b) R. E. Mark, J. Borch, *Handbook of physical testing of paper, Vol. 1*, CRC Press, Boca Raton, FL, **2001**; c) T. Unander, H.-E. Nilsson, *IEEE Sens. J.* **2009**, *9*, 922–928; d) T. Unander, J. Sidén, H.-E. Nilsson, *IEEE Sens. J.* **2011**, *11*, 3009–3018.
- [17] A. C. Glavan, D. C. Christodouleas, B. Mosadegh, H. D. Yu, B. S. Smith, J. Lessing, M. T. Fernández-Abedul, G. M. Whitesides, *Anal. Chem.* **2014**, *86*, 11999–12007.
- [18] I. M. Hutten, *Handbook of nonwoven media*, Elsevier, Amsterdam, **2007**.
- [19] R. B. Roe, *J. Am. Ceram. Soc.* **1919**, *2*, 69–73.
- [20] W. Dodds, L. Stutzman, B. Sollami, *Industrial & Engineering Chemistry, Chemical & Engineering Data Series* **1956**, *1*, 92–95; Engineering Chemistry, Chemical & Engineering Data Series **1956**, *1*, 92–95.
- [21] S. W. Smith, *The Scientist and Engineer's Guide to Digital Signal Processing*, California Technical Publishing, San Diego, **1997**.
- [22] a) F. Marvasti, A. Amini, F. Haddadi, M. Soltanolkotabi, B. H. Khalaj, A. Aldroubi, S. Sanei, J. A. Chambers, *EURASIP J. Adv. Sig. Proc.* **2012**, *2012*, 44; b) D. J. Holland, L. F. Gladden, *Angew. Chem. Int. Ed.* **2014**, *53*, 13330–13340; *Angew. Chem.* **2014**, *126*, 13546–13557.
- [23] Y. Y. Broza, P. Mochalski, V. Ruzsanyi, A. Amann, H. Haick, *Angew. Chem. Int. Ed.* **2015**, *54*, 11036–11048; *Angew. Chem.* **2015**, *127*, 11188–11201.

Received: December 21, 2015  
Published online: April 5, 2016